

Fig. 7 Transonic lateral stability characteristics of the Viking configuration.

rule, one should therefore avoid "tuning" one's predictions to agree with experimental results obtained in ground test facilities.

Acknowledgment

This work was supported by the Independent Development Program of Lockheed Missiles & Space Company, Inc., Sunnyvale, CA.

References

- Ericsson, L. E., and Reding, J. P., "Unsteady Aerodynamic Analysis of Space Shuttle Vehicles. Part II: Steady and Unsteady Aerodynamics of Sharp-Edged Delta Wings," NASA CR-124423, Aug. 1973.
- Ericsson, L. E., and King, H. H. C., "Rapid Prediction of Slender-Wing Aircraft Dynamics," AIAA Paper 90-3037, Aug. 1990.
- Wendtz, W. H., Jr., "Effects of Leading-Edge Camber on Low-Speed Characteristics of Slender Delta Wings," NASA CR-2002, Oct. 1972.
- Polhamus, E. C., "Predictions of Vortex-Lift Characteristics by a Leading-Edge-Suction Analogy," *Journal of Aircraft*, Vol. 8, April 1971, pp. 193-199.
- Ericsson, L. E., "Another Look at High-Alpha Support Interference," AIAA Paper 90-0188, Jan. 1990.
- Creel, T. R., Jr., and Penland, J. A., "Low Speed Aerodynamic Characteristics of a Hypersonic Research Airplane Concept Having a 70° Swept Delta Wing," NASA TMX-71974, Aug. 1974.
- Fox, C. H., Jr., Luckring, J. M., Morgan, H. L., Jr., and Huffman, J. K., "Subsonic Longitudinal and Lateral-Directional Static Aerodynamic Characteristics of a Slender Wing-Body Configuration," NASA TM-1011, Feb. 1988.
- Paulson, J. W., and Shanks, R. E., "Investigation of Low-Subsonic Flight Characteristics of a Model of a Hypersonic Boost-Glide Configuration Having a 78° Delta Wing," NASA TN D-894, May 1961.
- Davenport, E. E., "Aerodynamic Characteristics of Three Slender Sharp-Edge 74° Swept Wings at Subsonic, Transonic, and Supersonic Mach Numbers," NASA TN D-7631, Aug. 1974.
- Ehn, G., "Measurements of Static Stability Coefficients of an Ogive Delta Wing Model at Transonic and Supersonic Speeds," *The Aeronautical Research Institute of Sweden*, Bromma, Sweden, AU-876, Feb. 1974.
- Beyers, M. E., "Some Recent NAE Experience of Support Interference in Dynamic Tests," NRC NAE LTR-UA-83, Ottawa, Canada, Nov. 1985.

Walter B. Sturek
Associate Editor

Titan Improvement Study: Hydrogen Core Stages

James A. Martin*
NASA Langley Research Center,
Hampton, Virginia 23665

Introduction

THE Titan launch vehicle has had a long and successful history of placing both manned and unmanned payloads into orbit. It has been used for low Earth orbit (LEO), geosynchronous Earth orbit (GEO), and interplanetary launches. Several upper stages have been used but the Centaur is the upper stage that provides the greatest capability. The core stages have been used with and without the solid-rocket motors, and two sizes of solid-rocket motors have been developed. Titans have been launched from the east coast into easterly orbits and from the west coast into polar orbits. Except for the Saturn vehicles, which are no longer in use, the Titan has the greatest payload capability of any expendable launch vehicle in the free world.

As needs for greater payload capability or reduced costs appear, improvements of the Titan launch vehicle should be considered as an alternative to new designs. An incremental approach to improvements has the advantages of incremental development costs, confidence in the performance of the parts continuing to be used, and increasing production rates of the parts being used by both the new version and versions continuing in the inventory. The Titan is a good candidate for improvement because the core stages use storable propellants, which are toxic, expensive, and less energetic than hydrogen and oxygen.

Two possible improvements to the Titan/Centaur were considered, as shown in Fig. 1. First, a new hydrogen/oxygen stage II was studied that replaces both the Core II and the Centaur. Next, a new hydrogen/oxygen stage I was considered that replaces the current Core I stage. The new stage II was also examined as an orbit transfer vehicle for use with a new launch vehicle.

This study was conducted as part of continuing studies of advanced rocket engines. The Titan improvement could be one of several justifications for a new hydrogen/oxygen rocket engine with 500-1000 kN thrust.

Standard Titan/Centaur Capability

The ideal-velocity capability of the Titan/Centaur was calculated for various payloads, based on data from Ref. 1. The results are shown in Fig. 2 in an accumulative fashion. The solid rocket motors provide between 2.1 and 2.4 km/s of ideal velocity. The Core I stage adds about 2.4-3.0 km/s. The Core II stage contributes about 2.7 km/s with no payload and about one-half as much with a payload of 32 Mg. The Centaur provides over 8.8 km/s with no payload, but this decreases rapidly to less than 1.5 km/s with a payload of 32 Mg. The Centaur stage is not used for payloads over 7 Mg.

Received Oct. 4, 1989; revision received April 2, 1990. Copyright © 1990 by the American Institute of Aeronautics and Astronautics, Inc. No copyright is asserted in the United States under Title 17, U.S. Code. The U.S. Government has a royalty-free license to exercise all rights under the copyright claimed herein for Governmental purposes. All other rights are reserved by the copyright owner.

*Aerospace Engineer, Space Systems Division. Associate Fellow AIAA.

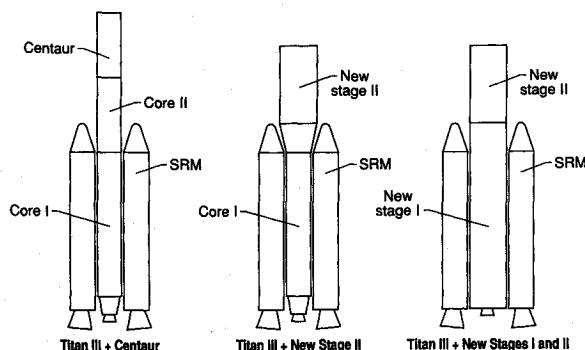


Fig. 1 Titan improvement options.

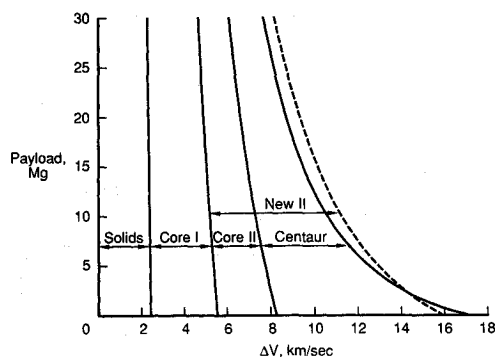


Fig. 2 Effect of new stage II.

New Hydrogen/Oxygen Stage II

The new hydrogen/oxygen stage II was designed with a gross mass of 51.7 Mg with no payload, equal to that of the Titan III Core II and Centaur combined. Of this mass, 6.9 Mg is jettisoned before ignition, corresponding to the insulation and shroud mass of the Centaur that is jettisoned before ignition. The remaining inert mass of the new stage II was estimated to be 4.4 Mg.

The engine for the new stage II was assumed to be an expander cycle. An expander cycle uses heat collected by cooling the combustion chamber to drive the pumps. With a thrust level of 667 kN, a mixture ratio of 6.0, and an area ratio of 70, the maximum chamber pressure was calculated to be over 8.9 MPa if a copper alloy material is used in the chamber. The chamber pressure was assumed to be 8.3 MPa, and the specific impulse was calculated to be 459 s. A lower thrust level than 667 kN might be selected for the new stage II, particularly if two engines are used. The lower thrust level would allow a greater maximum chamber pressure, which would increase the specific impulse. Therefore, the results presented are conservative.

Results with the new stage II are shown in Fig. 2, in addition to the standard Titan/Centaur results. Except for payloads of less than 2.27 Mg, the new stage II provides an increased performance. Figure 3 shows the same data with an indication of the ideal velocity required for LEO and GEO missions. The payload to GEO is increased slightly, and the payload to LEO is about 22.7 Mg, which is considerably more than any current Titan provides.

The new stage II might provide a cost advantage over the standard Titan/Centaur because it would have one less stage. It could also have an advantage in payload mating. The new stage could be designed with a larger diameter than the current 3 m of the Core II, which would allow better mating to payload shrouds of large payloads up to 22.7 Mg. The full diameter of the solid rocket motors and the Core I end at the same height, which would allow a conical adapter for a larger diameter new stage II to fit between the solid rocket motors, as shown in Fig. 1. Propellant handling problems would be no

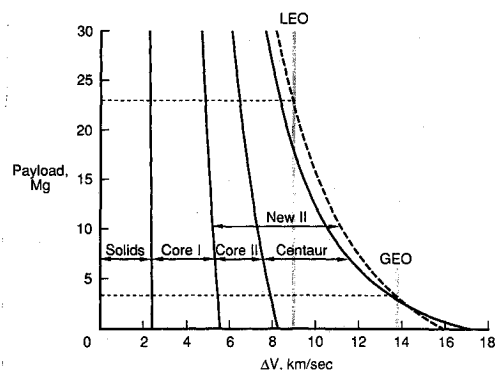


Fig. 3 Effect of new stage II.

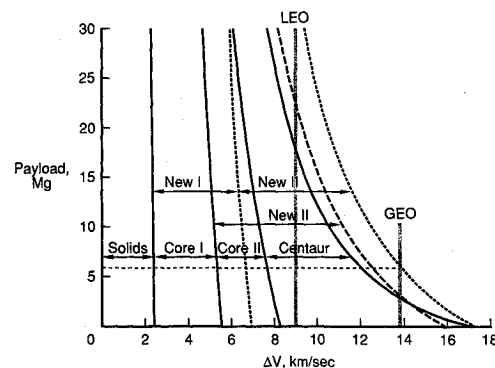


Fig. 4 Effect of new stage I.

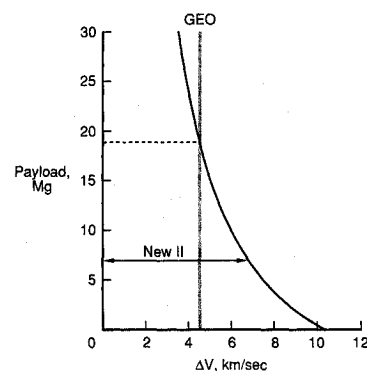


Fig. 5 New stage II as orbit transfer vehicle.

different because both hydrogen/oxygen and storables would be used.

The analysis was based on ideal velocities with no change in losses. The drag might increase because of the larger diameter new stage II, but many payloads already use a shroud with a larger diameter than the Core II. The gravity losses would depend on the thrust level selected.

New Hydrogen/Oxygen Stage I

A new hydrogen/oxygen stage I has also been analyzed in a similar manner to the new stage II. The gross mass of the new stage I was assumed to be 128 Mg, the same as the standard Titan III Core I. The inert mass was estimated to be 13.6 Mg, based on the Saturn S-IVB stage as used in the Saturn 1B.¹

The same engine is used for the new stage I that is used for the new stage II. The thrust needed would be greater by a factor of three or four. If one engine is used on stage II, three or four could be used on stage I. There may be some justification for using two engines on stage II for engine-out capability. Even so, each engine should not be much smaller or the stage would not have enough thrust with one engine out. With two smaller engines on stage II, stage I might need up to six en-

gines, but this would not be excessive with expander-cycle engines and would provide good engine-out capability.

Results with the new stage I are shown in Fig. 4 overlaid on Fig. 2. A significantly increased capability is provided at all payloads. Figure 4 also shows the requirements for the LEO and GEO missions. The payload to GEO is about 5.4 Mg, and the payload to LEO is over 31.7 Mg. Propellant handling problems would be reduced because the storables would be eliminated.

New Stage II as an Orbit Transfer Vehicle

Figure 5 shows the capability of the new stage II alone. This allows consideration of the stage as an orbital transfer vehicle, assuming it has been placed in a low-altitude easterly orbit by another launch vehicle, such as the Advanced Launch System (ALS). The stage has the capability to place about 18.1 Mg of payload in GEO. This would require 70 Mg to be placed in LEO by the launch vehicle, which is in the range being considered by the ALS studies.

Concluding Remarks

Significant improvements to the standard Titan/Centaur capability can be achieved by developing one or two new hydrogen stages requiring engines with a thrust level of about 667 kN or less. The new stage II might also be useful as an orbital transfer vehicle.

Reference

- ¹Valesco, T. E., Huang, R. S., and Edwards, R. G., "Characteristics of Launch Vehicles Selected for High Speed Reentry Testing Studies," LTV Aerospace Corp., NASA CR-66248, April 1967.

Hypersonic Nonequilibrium Viscous Solutions over Slender Bodies

E. V. Zoby*

NASA Langley Research Center,
Hampton, Virginia 23665

K. P. Lee†

Vigyan Research Associates, Inc.,
Hampton, Virginia 23666
and

R. N. Gupta*

NASA Langley Research Center,
Hampton, Virginia 23665

Introduction

THE low-altitude ascent phase of a transatmospheric vehicle¹ should provide conditions that define the major thermal protection requirements of the vehicle. The higher altitude phase and entry conditions are probably characterized by nonequilibrium heating conditions. For these conditions, the designer must determine if an active cooling method is required,

in particular, for leading edges, and the resulting weight increase. The leading edges (nose, tail, wings) and adjacent downstream surfaces represent a large surface region for these vehicles, and the additional coolant weight requirements may be important to vehicle performance.

Although the importance of nonequilibrium flow has been known for some time, its benefits to flight applications for a low catalytic surface were first illustrated by the heating rates measured during the initial flights of the Space Shuttle. As a result of the data from those early Shuttle flights, the effect of nonequilibrium chemistry on the Shuttle thermal environment is well documented.^{2,3} However, the altitude-velocity range and vehicle attitude and bluntness ranges, for which nonequilibrium chemistry impacts laminar heat transfer over long slender bodies, are not well established by experimental or computational results.

A recent parametric study⁴ was conducted to increase the computational data base on the nonequilibrium aerothermal environment for slender vehicles at hypersonic speeds. The study included the variation in altitude-velocity conditions, blunted cone half-angles, and nose bluntness. The effects of vehicle attitude and surface temperature were also considered. The laminar heat transfer calculations were presented as a ratio of the noncatalytic to fully catalytic heating rates to illustrate the maximum potential for a heating reduction in dissociated nonequilibrium flow. A smaller value of the ratio implies a larger potential for a heating reduction in nonequilibrium flow. The heating rate for a finite-catalytic wall would be greater than the value computed for a noncatalytic wall, and, thus, the actual heat reduction would be less than the values presented in Ref. 4. As the flow chemistry tends toward a frozen or equilibrium state, the ratio approaches one, and benefits of a finite-catalytic surface would not be realized.

The purpose of this technical Note is to provide an extension of the Ref. 4 investigation. Smaller nose radii are included for the cone half-angle range; individual nonequilibrium stagnation heating rates are presented at an ascent condition as a function of nose radius and also for an entry trajectory to demonstrate actual heating reductions; and the corresponding equilibrium heating predictions are presented to indicate the degree of conservatism present for such an assumption.

Analysis

For a complete detailed analysis, a Navier-Stokes (NS) method may be desirable, but the NS solution procedures require prohibitive computer run times and storage requirements for a parametric study over long bodies. The viscous shock-layer (VSL) equations, a subset of the NS equations, are obtained by retaining terms up to second-order in the inverse square root of the Reynolds number. The VSL method has been used extensively to study the effect of various physical phenomena (such as coupled radiation and ablation, turbulence, and nonequilibrium chemistry) on flowfield computations. The flow governing equations, boundary conditions, chemical kinetics thermodynamic and transport properties, and solution techniques for the VSL method of this study are presented in detail in Ref. 5.

Results and Discussion

The parametric study⁴ included cone half-angles of 6, 10, and 20 deg with corresponding nose radius range of 0.125, 0.5, and 0.75 ft. For this Note, the heating-reduction ratio is presented as a function of wetted distance over a 6 deg cone for a nose radii range from 0.05 to 0.75 ft. The computed ratio is also presented for a 0.25 ft radius to provide a better understanding of the heating trend with nose radius. The calculations were obtained at an altitude of 175,000 ft for a free-stream Mach number of 25 and a 2260 R wall temperature. A value of the heat-reduction ratio of less than 50% is obtained at running lengths equal to at least 14 ft for the larger nose

Received Nov. 21, 1990; revision received Dec. 13, 1991; accepted for publication Jan. 19, 1991. Copyright © 1991 by the American Institute of Aeronautics and Astronautics, Inc. No copyright is asserted in the United States under Title 17, U.S. Code. The U.S. Government has a royalty-free license to exercise all rights under the copyright claimed herein for Governmental purposes. All other rights are reserved by the copyright owner.

*Aero-Space Technologist, Aerothermodynamics Branch, Space Systems Division. Associate Fellow AIAA.

† Research Scientist. Member AIAA.